



Tempol ameliorates polycystic ovary syndrome through attenuating intestinal oxidative stress and modulating of gut microbiota composition-serum metabolites interaction

Tianhe Li^a, Tingting Zhang^a, Huimin Gao^a, Ruixia Liu^a, Muqing Gu^a, Yuxi Yang^a, Tianyu Cui^a, Zhongbing Lu^{b,*,**}, Chenghong Yin^{a,*}

^a Beijing Obstetrics and Gynecology Hospital, Capital Medical University, Beijing Maternal and Child Health Care Hospital, Beijing, 100026, China

^b College of Life Sciences, University of Chinese Academy of Sciences, Beijing, 100049, China

ARTICLE INFO

Keywords:

Polycystic ovary syndrome
Tempol
Gut microbiota
Metabolites

ABSTRACT

Polycystic ovary syndrome (PCOS) is a complex endocrine and metabolic disorder, which is often accompanied by oxidative stress. Tempol, a superoxide dismutase mimetic, protects against several diseases caused by oxidative stress. However, the effect of tempol on PCOS has not been investigated. The present study demonstrated the alleviation of ovarian dysfunction and glucose tolerance in dehydroepiandrosterone (DHEA)-induced PCOS rats treated with tempol. Tempol significantly reduced the intestinal oxidative stress in PCOS rats without affecting the ovarian redox rate. The 16S rDNA sequencing of the intestinal microbiome and non-targeted metabolomics analysis indicated significant differences in gut microbiota composition and serum metabolite profiles between the control and PCOS rats, and most of these differences were reduced after tempol intervention. Tempol alters the gut microbiome by increasing the abundance of genus *Ruminococcus_1* and by decreasing the abundance of *Ruminococcus_2*, *Staphylococcus*, *Ideonella*, and *Corynebacterium* genera. Tempol also attenuates the reduction of serum bile acid and stachyose levels in PCOS rats, and the serum stachyose level was significantly correlated with the abundance of 15 genera, particularly *Ruminococcus_1* and *Ruminococcus_2*. Moreover, stachyose administration improved ovarian dysfunction in PCOS rats. Thus, our data indicate that tempol ameliorates PCOS phenotype by reducing intestinal oxidative stress, restoring gut dysbiosis, and modulating the interaction between gut microbiota and host metabolite. Therefore, tempol intervention is a potential therapeutic approach for PCOS.

1. Introduction

Polycystic ovary syndrome (PCOS) is a common endocrine disorder that affects 6%–10% of women of reproductive age [1,2]. The primary characteristics of PCOS include androgen excess, ovulatory dysfunction and polycystic ovarian morphology [3]. Additionally, PCOS is often accompanied by metabolic disorders such as insulin resistance (IR), hyperglycemia, and obesity [4]. Although PCOS has been studied for a long time, its etiology and pathophysiology remain unclear.

Numerous studies have demonstrated that excessive production of reactive oxygen species (ROS), progressive reduction of the antioxidant capacity, and elevation of circulating oxidative stress biomarkers in patients with PCOS [5,6], which indicate that oxidative stress is

involved in the PCOS pathophysiology. A study by Masjedi et al. demonstrated a significant reduction in superoxide dismutase (SOD) activity in serum and follicular fluid of patient with PCOS [7], whereas another study by Sun et al. demonstrated the association of glutathione peroxidase 1 (GPx1) P198L genetic polymorphism with PCOS risk in Chinese women [8]. Because oxidative stress is reflected as an imbalance between pro- and antioxidants, several antioxidants, such as vitamin C [9], vitamin E [10,11] and MitoQ10 [12] have been recognized as potential therapeutics for PCOS. A recent cohort study exhibited that, a short-term supplementation of vitamin E in patients with PCOS can reduce oxidative stress, and reduce exogenous human menopausal gonadotropin dosage in the ovulation induction cycle [13]. Tempol is a stable SOD mimetic that can be used as a chemical antioxidant to treat diseases caused by oxidative stress [14]. However, the effect of tempol

* Corresponding author. Beijing Obstetrics and Gynecology Hospital, Capital Medical University, No 251, Yaojiayuanlu, Chaoyang District, Beijing, 100026, China.

** Corresponding author. College of Life Sciences, University of Chinese Academy of Sciences, NO 19A, Yuquanlu, Shijingshan District, Beijing, 100049, China.

E-mail addresses: luzhongbing@ucas.ac.cn (Z. Lu), modscn@126.com, yinchh@ccmu.edu.cn (C. Yin).

<https://doi.org/10.1016/j.redox.2021.101886>

Received 20 September 2020; Received in revised form 8 December 2020; Accepted 28 January 2021

Available online 3 February 2021

2213-2317/© 2021 The Authors.

Published by Elsevier B.V. This is an open access article under the CC BY-NC-ND license

(<http://creativecommons.org/licenses/by-nc-nd/4.0/>).

| Abbreviations | |
|---------------|---|
| 3'-NT | 3-nitrotyrosine |
| ACE | abundance-based coverage estimator |
| AGEs | advanced glycation end products |
| DHEA | dehydroepiandrosterone |
| eE2 | 17 α -ethynylestradiol |
| FXR | farnesoid X receptor |
| FSH | follicle stimulating hormone |
| GDCA | glycodeoxycholic acid |
| GPBAR1 | G protein-coupled bile acid receptor 1 |
| GPx1 | glutathione peroxidase 1 |
| GSH | glutathione |
| H&E | hematoxylin and eosin |
| HFD | high fat diet |
| HOMA-IR | homeostatic model assessment of insulin resistance |
| IR | insulin resistance |
| ITTs | insulin tolerance tests |
| LH | luteinizing hormone |
| MDA | malonyldialdehyde |
| OGTTs | oral glucose tolerance tests |
| OPLS-DA | orthogonal projections to latent structures-discriminant analysis |
| PCoA | principal coordinate analysis |
| PCOS | polycystic ovary syndrome |
| PRGE | progesterone |
| ROS | reactive oxygen species |
| SOD | superoxide dismutase |
| T-AOC | total antioxidant capacity |
| TUNEL | terminal deoxynucleotidyl transferase dUTP nick end labeling |
| UPGMA | unweighted pair group method with arithmetic mean |

on PCOS has not been investigated.

Evidence suggests that PCOS is inextricably linked to gut microbiota that plays a vital role in the metabolic and immune systems [15]. Considerable changes in the composition of gut microbiota have been observed in patients with PCOS [16]. The restoration of gut microbiota dysbiosis through dietary probiotic inulin supplementation [17] or α -linolenic acid-rich flaxseed oil [18] contributes to the amelioration of PCOS. It has been proposed that IR, metabolic abnormality, and sex hormone concentrations in women with PCOS may affect the diversity and composition of gut microbiota. On the other hand, gut microbiota dysbiosis could contribute to IR and obesity in patients with PCOS because of the stimulation of inflammatory activities and disruption of energy balance [19,20]. Similarly, the alteration in composition of gut microbiota may induce excessive ROS production in the gastrointestinal system [21]. Antioxidant intervention could overcome gut dysbiosis in some disease models, streptozotocin-induced diabetic rats with peripheral neuropathy [22], diet-induced obese rats [23], and ulcerative colitis models [24]. Tempol alters gut microbiome in high fat diet (HFD)-fed mice, leading to the inhibition of the intestinal farnesoid X receptor (FXR) signaling and decreased obesity [25]. However, the effect of tempol on gut microbiota in PCOS models has not been investigated.

In the present study, we investigated the protective effect of tempol on ovarian function, oxidative stress, IR and gut microbial compositions in dehydroepiandrosterone (DHEA)-induced PCOS rat models. We also performed non-targeted metabolomics to investigate the association between gut microbiota and serum metabolites in these animals.

2. Materials and methods

2.1. Antibodies and reagents

Antibodies against Cleaved Caspase-3, SOD1, SOD2 and β -actin were purchased from Cell Signaling Technology (#9661, #37385, #13141, #12262, Danvers, MA, USA). Tempol was purchased from Selleck Chemicals LLC (#S2910, Houston, TX, USA). Kits for terminal deoxynucleotidyl transferase dUTP nick end labeling (TUNEL) staining, total antioxidant capacity (T-AOC), malonyldialdehyde (MDA) and SOD activity assay were purchased from Beyotime Institute of Biotechnology (#C1091, #S0119, #S0131S, #S0101, Shanghai, China). 3-nitrotyrosine (3'-NT) and advanced glycation end products (AGEs) ELISA kits were purchased BlueGene Biotech (#E02A0670, #E02A002 Shanghai, China). Wright's stain kit was obtained from Coolaber Biotechnology Co. Ltd (#SL7030, Beijing, China). All other chemicals made in China were of analytical grade.

2.2. Experimental animals

Animal studies were performed in accordance with the Principles of Laboratory Animal Care (NIH publications No. 8023, revised 1978) and with approval by the Ethics Committee of Pony Testing International Group. Rats were maintained under standard housing conditions (free access to food and water in a temperature and humidity controlled, 12-h light:12-h dark environment) at the Pony Testing International Group Co., Ltd (Beijing, China).

To induce PCOS, 3-week-old female prepuberal Sprague Dawley rats were daily subcutaneously injection of 60 mg/kg DHEA (dissolved in 0.2 ml of sesame oil). The control rats were daily injected with 0.2 ml sesame oil. After treatment for 21 days, the rats were treated with 0.2 ml phosphate-buffered saline (PBS), 30 mg/kg tempol or 200 mg/kg stachyose (tempol or stachyose was dissolved in 0.2 ml PBS) by intraperitoneal injection for 12 days. Then, part of rats was sacrificed and serum samples, ovary and intestine tissues were collected. At this time, fresh feces samples were taken from the colons of all rats, and then transferred into 5 ml sterile EP tubes. These tubes were rapidly snap-frozen in liquid nitrogen, and stored at -80°C . The rest of rats were used for mean daily food intake measurement and estrous cycle determination, in the next 7 or 10 days.

2.3. Estrous cycle determination

As previously described [15], vaginal smears were taken daily at same time from the 1st to 10th day after the second treatment. The stage of the estrous cycle was determined by microscopic analysis of the predominant cell type in vaginal smears using Wright's stain kit.

2.4. Measurement of serum biochemical markers

Serum testosterone, 17 α -ethynylestradiol (eE2), luteinizing hormone (LH), progesterone (PRGE) and follicle stimulating hormone (FSH) levels were determined by radioimmunoassay (XH6080, Xi'an, China). Serum total bile acid were measured using the AU480 chemistry analyzer (Beckman, American). Blood glucose and serum insulin levels were measured using an Accu-Chek[®] glucometer (Roche Diagnostics, Indianapolis, IN, USA) and Rat Ultrasensitive Insulin ELISA kit (#80-INSRT-E01, ALPCO Diagnostics, Salem, NH, USA), respectively. The homeostatic model assessment of IR (HOMA-IR) index was calculated using the formula: [fasting glucose levels (mmol/l)] * [fasting serum insulin (IU/ml)]/22.5. As previously described [26], the oral glucose tolerance tests (OGTTs) were performed by oral gavage of 2 g/kg of glucose after overnight fasting. The insulin tolerance tests (ITTs) were performed via intraperitoneal injection of 0.75 U/kg of insulin after

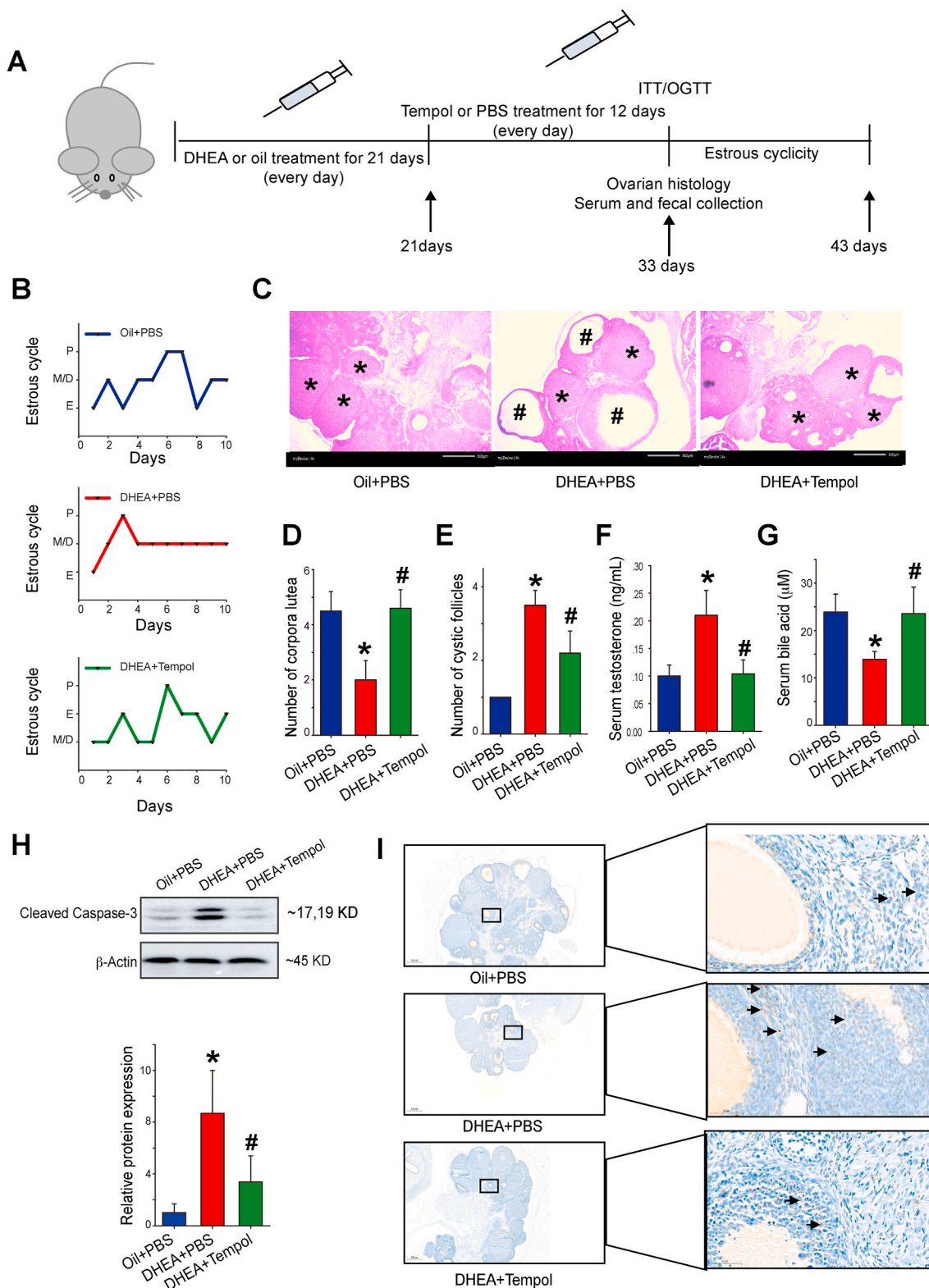


Fig. 1. Tempol alleviates ovarian dysfunction in dehydroepiandrosterone (DHEA)-induced PCOS rats. The group assignments and time line of the experimental process are illustrated in diagram (A). Female rats were treated with DHEA or sesame oil for 21 days, followed by an intraperitoneal injection of tempol or PBS for another 12 days. The estrous cycles were determined after another 10 days ($N = 3$) (B). Representative ovary sections were stained with hematoxylin and eosin (scale bar = 500 μm; * indicates cystic follicles; # indicates corpora lutea) (C) and the number of corpora lutea (D) and cystic follicles (E) was determined from these stained sections ($N = 4$). Serum testosterone and bile acid levels were measured using radioimmunoassay method and enzyme-linked immunosorbent assay kit, respectively (F, G) ($N = 7$). Lysates of ovary tissue were examined using Western blotting to determine the expression level of cleaved caspase 3, and β-actin was used as the loading control (H) ($N = 3$). Representative ovary sections were also stained with TUNEL kits (scale bar = 500 μm, arrows point to TUNEL-positive cells) (I). Data are presented as mean ± standard error of mean (SEM); * indicates significance ($p < 0.05$) compared with the oil + PBS group, # indicates significance ($p < 0.05$) compared with the DHEA + PBS group.

fasting for 4 h. At least 7 rats/group were used for these experiments.

2.5. Tissue processing

Rat ovaries were harvested, washed, and fixed with formalin and embedded in paraffin. Ovary sections (5 μ m) were stained with hematoxylin and eosin (H&E) or TUNEL kits respectively. At least 4 rats per group were used for these experiments.

2.6. Western blotting

Ovaries and intestinum were pulverized, and proteins were extracted using buffer (50 mM Tris-HCl, 150 mM NaCl, 100 μ g/ml phenylmethylsulfonyl fluoride, protease and phosphatase inhibitor cocktails, and 1% Triton X-100) on ice for 30 min. After centrifugation at 12,000 g for 20 min at 4 $^{\circ}$ C, the supernatant was used for Western blot analysis.

2.7. Serum metabolic profiles analysis

100 μ L of serum was mixed with 400 μ L extract solution (acetonitrile:methanol = 1: 1) containing isotopically-labelled internal standard mixture in a tube. After 30 s vortex, the samples were sonicated for 5 min in ice-water bath. Then the samples were incubated at -40° C for 1 h and centrifuged at 12000 rpm for 15 min at 4 $^{\circ}$ C. 400 μ L of supernatant was transferred to a fresh tube and dried in a vacuum concentrator at 37 $^{\circ}$ C. Then, the dried samples were reconstituted in 200 μ L of 50% acetonitrile by sonication on ice for 10 min. The constitution was then centrifuged at 13000 rpm for 15 min at 4 $^{\circ}$ C, and 75 μ L of supernatant was transferred to a fresh glass vial for LC/MS analysis. The quality control sample was prepared by mixing an equal aliquot of the supernatants from all of the samples.

The UHPLC separation was carried out using a ExionLC Infinity series UHPLC System (AB Sciex, Boston, MA, USA), equipped with a UPLC BEH Amide column (2.1 * 100 mm, 1.7 μ m, Waters). The mobile phase consisted of 25 mmol/L ammonium acetate and 25 mmol/L ammonia hydroxide in water (pH = 9.75) (A) and acetonitrile (B). The analysis was carried with elution gradient as follows: 0–0.5 min, 95%B; 0.5–7.0 min, 95%–65% B; 7.0–8.0 min, 65%–40% B; 8.0–9.0 min, 40% B; 9.0–9.1 min, 40%–95% B; 9.1–12.0 min, 95% B. The column temperature was 25 $^{\circ}$ C. The TripleTOF 5600 mass spectrometry (AB Sciex) was used for MS/MS spectra acquisition on an information-dependent basis mode during an LC/MS experiment. In this mode, the acquisition software (Analyst TF 1.7, AB Sciex) continuously evaluates the full scan survey MS data as it collects and triggers the acquisition of MS/MS spectra depending on preselected criteria. In each cycle, the most intensive 12 precursor ions with intensity above 100 were chosen for MS/MS at collision energy of 30 eV. The cycle time was 0.56 s. ESI source conditions were set as following: Gas 1 as 60 psi, Gas 2 as 60 psi, Curtain Gas as 35 psi, Source Temperature as 600 $^{\circ}$ C, Declustering potential as 60 V, Ion Spray Voltage Floating as 5000 V or -4000 V in positive or negative modes, respectively.

2.8. Data processing

MS raw data (.wiff) files were converted to the mzXML format by ProteoWizard, and processed by R package XCMS (version 3.2). The process includes peak deconvolution, alignment and integration. Minfrac and cut off are set as 0.5 and 0.3 respectively. In-house MS2 database was applied for metabolites identification.

2.9. 16S rDNA gene sequencing

Total bacterial DNA were extracted from feces using the Power Soil DNA Isolation Kit (MO BIO Laboratories, Carlsbad, CA, USA) according to the manufacturer's protocol. DNA quality and quantity were assessed

by the ratios of 260 nm/280 nm and 260 nm/230 nm. Then DNA was stored at -80° C until further processing. The V3–V4 region of the bacterial 16S rRNA gene was amplified with the common primer pair (Forward primer, 5'-ACTCCTACGGGAGGCAGCA-3'; reverse primer, 5'-GGACTACHVGGGTWTCTAAT-3') combined with adapter sequences and barcode sequences. Thermal cycling conditions were as follows: an initial denaturation at 95 $^{\circ}$ C for 5 min, followed by 15 cycles at 95 $^{\circ}$ C for 1 min, 50 $^{\circ}$ C for 1 min and 72 $^{\circ}$ C for 1 min, with a final extension at 72 $^{\circ}$ C for 7 min. The PCR products from the first step PCR were purified through VAHTSTM DNA Clean Beads. A second round PCR was then performed in a 40 μ L reaction which contained 20 μ L 2 \times Phusion HF MM, 8 μ L ddH₂O, 10 μ M of each primer and 10 μ L PCR products from the first step. Thermal cycling conditions were as follows: an initial denaturation at 98 $^{\circ}$ C for 30s, followed by 10 cycles at 98 $^{\circ}$ C for 10s, 65 $^{\circ}$ C for 30 s min and 72 $^{\circ}$ C for 30s, with a final extension at 72 $^{\circ}$ C for 5 min. Finally, all PCR products were quantified by Quant-iT™ dsDNA HS Reagent and pooled together. High-throughput sequencing analysis of bacterial rRNA genes was performed on the purified, pooled sample using the Illumina HiSeq 2500 platform(2 \times 250 paired ends, San Diego, CA, USA).

2.10. Data and statistical analysis

All values are expressed as mean \pm standard error. Statistical significance was defined as $P < 0.05$. One-way analysis of variance (ANOVA) was used to test each variable for differences among three groups with StatView (SAS Institute Inc, Cary, NC, USA). If the analysis of variance demonstrated a significant effect, post hoc comparisons were made pairwise using Fisher's least significant difference test. For the nonparametric tests, the two-tailed Mann-Whitney test was used to evaluate statistical significance between three groups. Spearman correlation between the level of fecal metabolites and the relative abundance of genera was performed by the cor.test function from the stats R package. We only performed the correlation in those genera ($P < 0.05$) and metabolites ($P < 0.05$, VIP > 1), which were found to be statistically significant between groups.

3. Results

3.1. Tempol attenuates ovarian dysfunction and cell apoptosis in DHEA-induced PCOS rats

The experimental processes are illustrated in Fig. 1A. Since DHEA was dissolved in sesame oil during the experiment process, the sesame oil treated group was used as sham control. The rats were randomly divided into three groups, namely, oil + PBS, DHEA + PBS, and DHEA + tempol. The body weight and food intake at the end of experimental period (day 33) were nearly identical in these groups (Fig. S1). The estrous cycles were measured to determine the effect of DHEA and/or tempol on ovarian functions. Rats in the oil + PBS group exhibited regular estrous cycles of 4–5 days, whereas most rats in the DHEA + PBS group were in the diestrus phase (Fig. 1B). The estrous cycles disorder improved after tempol treatment (Fig. 1B). Afterwards, H&E staining was performed to determine the alteration of ovarian pathology in diverse groups. Ovaries in the oil + PBS group exhibited follicles and a few fresh corpora lutea during different developmental stages (Fig. 1C). The DHEA + PBS group exhibited a higher number of cystic follicles and a lower number of corpus luteum compared with the control group. On the other hand, tempol administration decreased the number of cystic follicles and increased the formation of corpus lutea (Fig. 1C–E). The serum levels of five sex steroid hormones, namely testosterone, eE2, LH, PRGE and FSH were measured subsequently. Serum testosterone levels were significantly higher in the DHEA + PBS group compared with the oil + PBS group. Tempol significantly decreased serum testosterone and eE2 levels but had no obvious effect on serum LH, PRGE, and FSH levels in PCOS rats (Fig. 1F, Fig. S2). The alternating bile acid metabolism has been observed in PCOS patients,

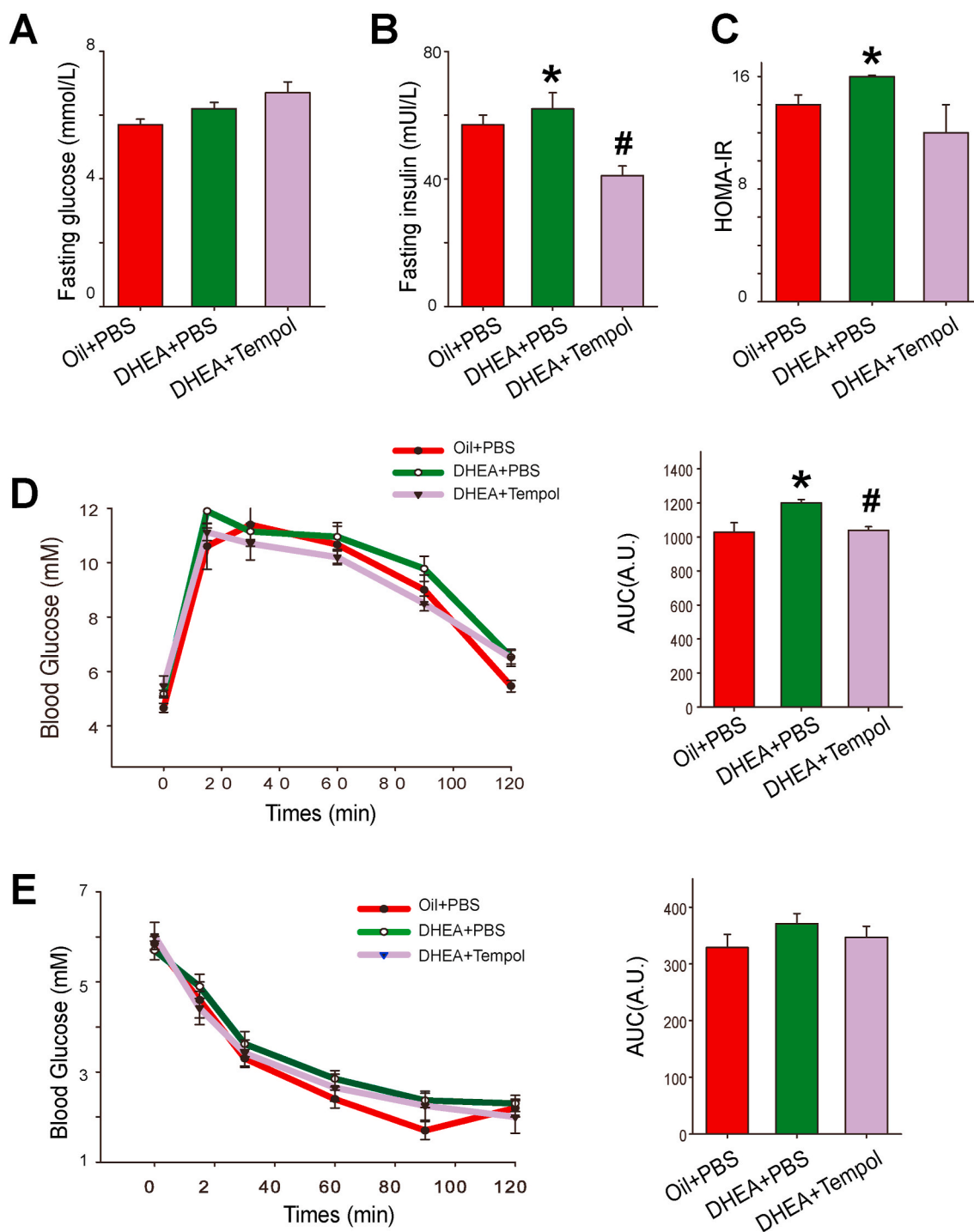


Fig. 2. Effects of tempol on glucose tolerance and insulin sensitivity in PCOS rats. After fasting for 12 h, the blood glucose (A) and serum insulin (B) levels in rats in the oil + PBS, DHEA + PBS, and DHEA + tempol groups were measured ($N = 7$). The homeostasis model assessment of insulin resistance (HOMA-IR) index was calculated as follows: (fasting glucose levels [mmol/L]) \times (fasting serum insulin [μ U/mL])/22.5 (C). Oral glucose tolerance tests (OGTTs) (D) and insulin tolerance tests (ITTs) (E) were performed on rats of all the three groups ($N = 7$). The corresponding area under the curve (AUC) of blood glucose levels in each group was calculated. Values are presented as means \pm SEM; * indicates significance ($p < 0.05$) compared with the oil + PBS group, # indicates significance ($p < 0.05$) compared with the DHEA + PBS group.

and bile acid administration improved insulin resistance, ovarian dysfunction and infertility in mice with PCOS [15]. Consistent with that finding, the serum bile acid levels were significantly reduced in DHEA-treated rats, and such reduction was diminished in rats of DHEA + tempol group (Fig. 1G). In the ovaries of rats in DHEA + PBS group, the expression of cleaved caspase-3 were increased, and this increase

was diminished by tempol administration (Fig. 1H). TUNEL staining revealed that tempol significantly decreased the proportion of apoptotic cells in DHEA-treated rats (Fig. 1I). Together, these results suggest that tempol ameliorated ovarian dysfunction and pathological damage of ovarian tissues in PCOS rats.

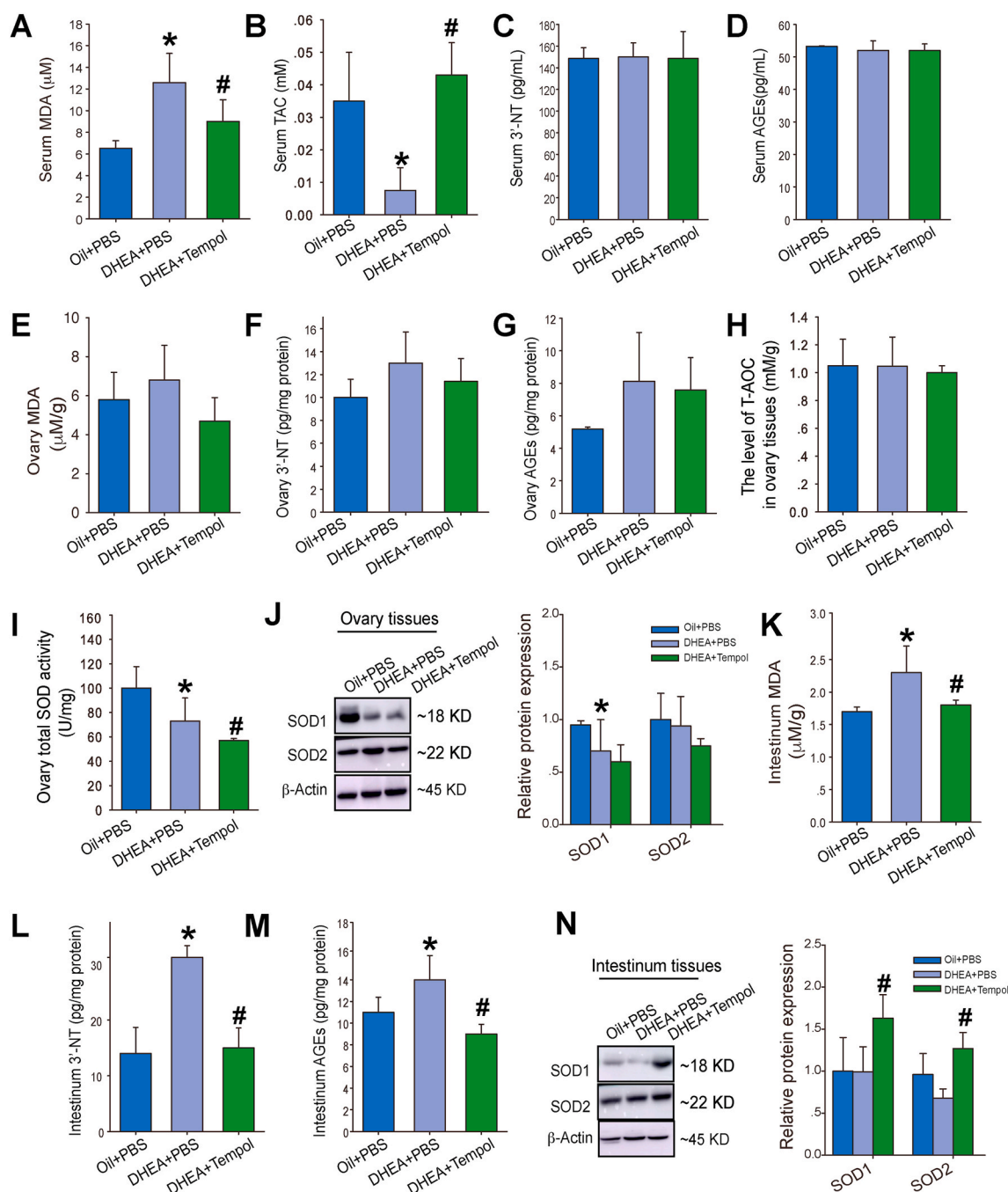


Fig. 3. Effects of tempol on systemic, ovarian, and intestinal oxidative stress in PCOS rats. The serum levels of malonyldialdehyde (MDA) (A), total antioxidant capacity (T-AOC) (B), 3'-NT (C), and advanced glycation end products (AGEs) (D) were measured ($N = 5$). The levels of MDA (E), 3'-NT (F), AGEs (G) and T-AOC (H), and SOD activity (I) in ovarian lysates were determined ($N = 5$). The protein levels of SOD1 and SOD2 in ovaries were determined using Western blotting (J) ($N = 5$). Intestinal tissue lysates were also used for the measurement of MDA (K), 3'-NT (L), and AGEs (M) levels, and SOD1 and SOD2 protein levels (N) ($N = 5$). Values are presented as means \pm SEM; * indicates significance ($p < 0.05$) compared with the oil + PBS group, # indicates significance ($p < 0.05$) compared with the DHEA + PBS group.

3.2. Tempol moderately ameliorates glucose tolerance in DHEA-induced PCOS rats

Because PCOS is closely associated with metabolic disorders, we assessed insulin sensitivity and glucose homeostasis in diverse groups. Although no significant difference was observed in fasting blood glucose levels, rats in the DHEA + PBS group displayed a higher fasting serum insulin level and higher HOMA-IR values than those in the oil + PBS group. Tempol significantly decreased fasting insulin levels, whereas it

was found to have no significant effect on fasting blood glucose level and HOMA-IR values in PCOS rats (Fig. 2A-C).

OGTTs revealed a delayed glucose clearance and increased area under the curve in PCOS rats, which indicate that DHEA treatment decreases glucose excretion capability. This impairment in glucose tolerance was improved by tempol administration (Fig. 2D). ITTs demonstrated that rats in all the three groups respond equally to insulin (Fig. 2E).

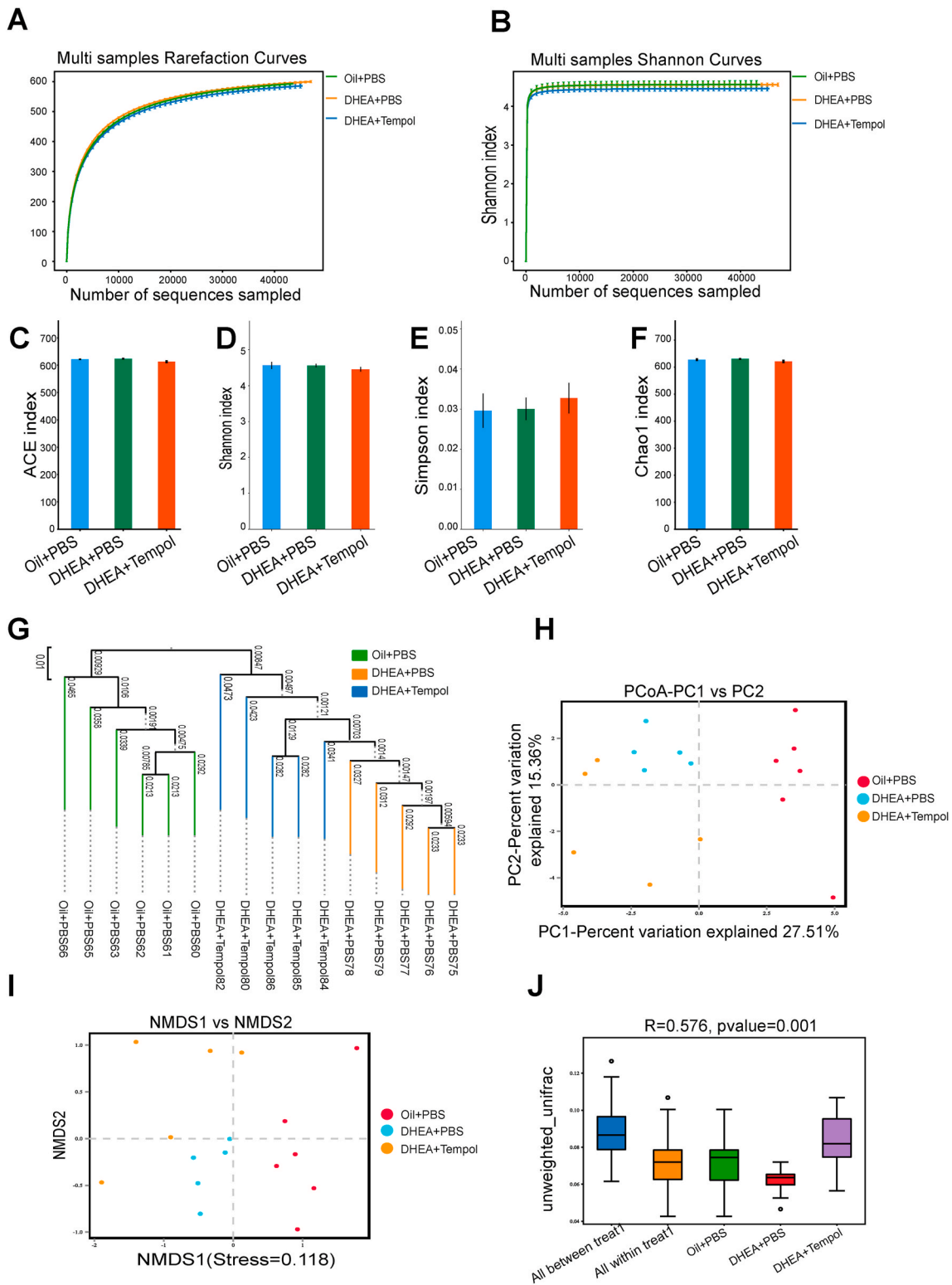


Fig. 4. Effect of Tempol on alpha diversity of gut microbiota. Analysis of gut microbial diversity was performed on the basis of 16S rDNA sequencing. Rarefaction curves (A) and Shannon index (B) are presented. ACE (C), Shannon index (D), Simpson index (E), and Chao1 index (F) were used to describe alpha diversity of gut bacterial assemblages in the rats receiving different treatments. Bacterial community compositional similarity was evaluated by beta diversity. Unweighted UPGMA of all samples was conducted on the basis of the Jaccard distance matrix (G). Plots of unweighted UniFrac-based PCoA (H) and nonmetric multidimensional scaling (NMDS) plots based on Jaccard dissimilarity (I) are presented. Analysis of similarities (Anosim) was used to detect differences between the groups (J). *N* = 5–6 rats per group.

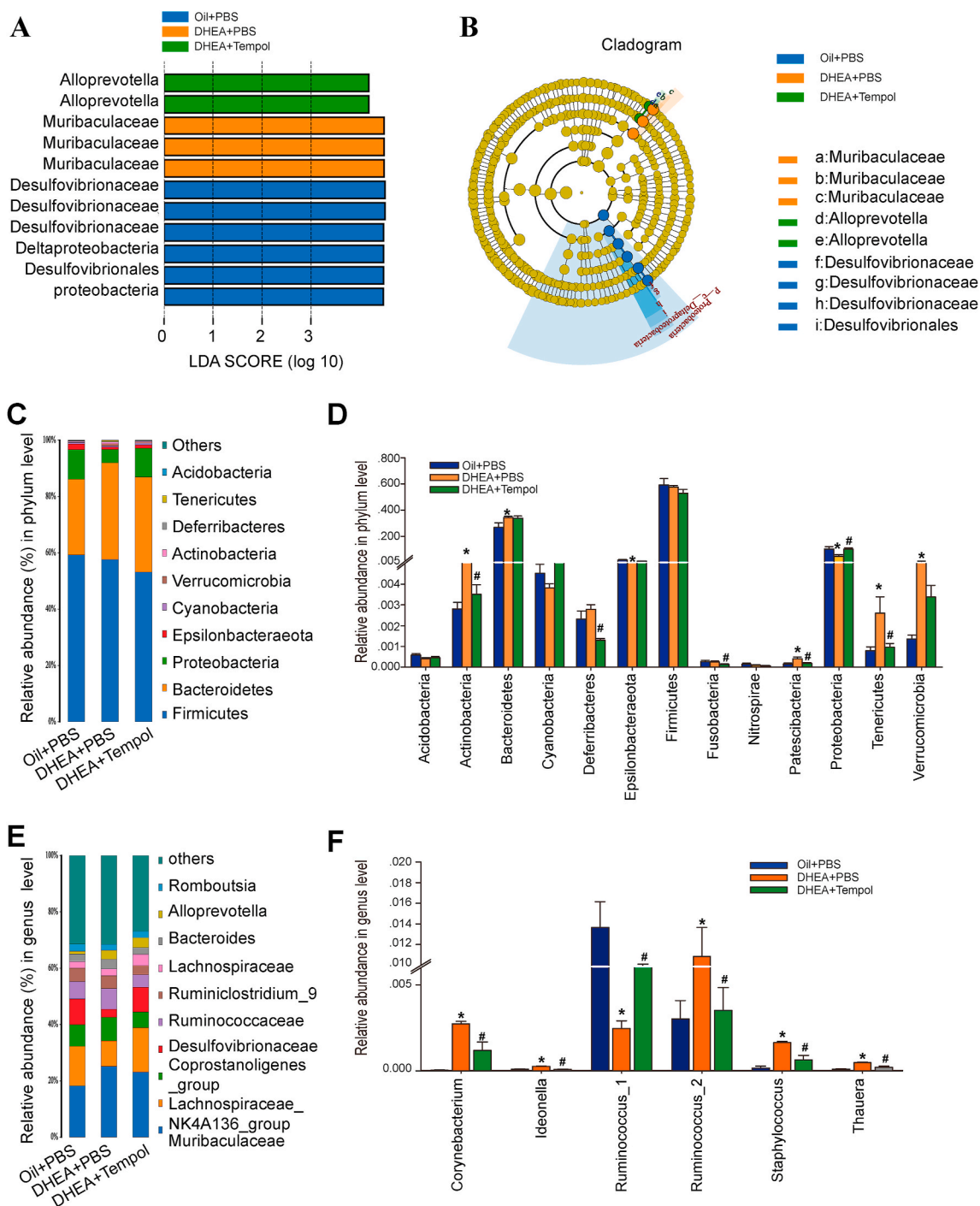


Fig. 5. Changes in the taxonomic composition of ileum microbial communities at the phylum and genus levels. Statistical differences in the levels of biomarkers between the oil + PBS, DHEA + PBS, and DHEA + tempol groups were identified using line discriminant analysis (LDA) effect size (LEfSe) method. Taxa enriched in oil + PBS (Blue), DHEA + PBS (Orange), and DHEA + Tempol (Green) groups are indicated by LDA scores. Only the taxa meeting an LDA significant threshold of four are displayed, and the length of histogram represents the influence of different species (A). Cladogram visualizes the output of LEfSe algorithm. Significantly distinct taxonomic nodes are colored and the branch areas are shaded according to the effect size of the taxa (B). The top ten bacteria, with maximum abundance of ileum bacteria at the phylum (C) and genus (E) levels. Significant changes in abundance at the phylum (D) and genus (F) levels. (Blue) taxa enriched in the Oil + PBS group; (Orange) taxa enriched in the DHEA + PBS group; (Green) taxa enriched in the DHEA + Tempol group; (Yellow) corresponding nodes of the taxa that were not significantly different between the groups (B). $N = 5-6$ rats per group, values are presented as means \pm SEM; * indicates significance ($p < 0.05$) when compared with the oil + PBS or DHEA + PBS groups. (For interpretation of the references to color in this figure legend, the reader is referred to the Web version of this article.)

3.3. Tempol ameliorates systemic and intestinal oxidative stress in PCOS rats

We measure the levels of oxidative stress biomarkers in serum to

determine the effects of DHEA and tempol on systemic oxidative stress. Rats in the DHEA + PBS group exhibited a significantly higher serum MDA level and lower levels of serum T-AOC than those in the oil + PBS group. Tempol administration significantly decreased the serum MDA

level and increased the serum T-AOC level in PCOS rats (Fig. 3A–B). DHEA treatment with or without tempol administration was found to have no effect on serum 3'-NT and AGEs levels (Fig. 3C–D).

We also determined the levels of oxidative stress biomarkers in ovary. Although the levels of MDA, 3'-NT, and AGEs were higher in the ovaries of PCOS rats than in those of the control rats, the difference was not statistically significant (Fig. 3E–G). Additionally, no significant decrease was observed in the T-AOC levels in the PCOS rats (Fig. 3H); however, the SOD activity was decreased in these rats (Fig. 3I). Western blotting analysis revealed a decrease in SOD1 expression, whereas SOD2 expression was unchanged in the ovaries of PCOS rats (Fig. 3J). Tempol administration demonstrated no obvious effect on the levels of these oxidative stress biomarkers and even decreased the ovarian SOD activity further in the PCOS rats (Fig. 3E–I), which indicate that tempol has no direct effect on ovarian oxidative stress.

Since gut microbiota plays an important role in the initiation and development of PCOS, we also investigated whether DHEA and tempol affect redox state in the intestinal tract. The intestinal MDA, 3'-NT, and AGEs levels were significantly higher in the PCOS rats than in the control rats, and the increase in oxidative biomarkers was attenuated by tempol administration (Fig. 3K–M). Moreover, tempol significantly increased the intestinal SOD1 and SOD2 expression in the PCOS rats (Fig. 3N). Thus, these results indicate that tempol lowers intestinal oxidative stress in PCOS rats.

3.4. Tempol attenuated gut microbiota dysbiosis in PCOS rats

Because tempol has a profound effect on intestinal oxidative stress, we performed 16S rDNA sequencing by using fecal samples to determine the effect of tempol on the composition and levels of gut microbiota in PCOS rats. The bacterial V3/V4 16S rDNA sequencing reads were obtained from 16 fecal samples, with an average of 74,377 validated tags per sample (with a minimum of 73,467 reads and a maximum of 75,513 reads) (Fig. S3). Additionally, the sample numbers, species richness, and evenness were analyzed by the species accumulation and rank abundance curve (Fig. S4), which demonstrated that the volume and quality of the fecal samples were adequate for sequencing and subsequent analysis. Subsequently, the abundance and diversity of the bacterial community were assessed by the rarefaction and Shannon curves (Fig. 4A–B), and four α -diversity indices, namely, abundance-based coverage estimator (ACE), Shannon, Simpson, and Chao1. The multiple sample rarefaction curves tended to be flat when the sequence number increased to 20,000, which indicated that the amount of sequencing data is reasonable (Fig. 4C–F). Similar results were observed in the multiple sample Shannon curves (Fig. 4G), which suggest that a majority of the sample diversity was covered by sequencing. Interestingly, the results from the rarefaction and Shannon curves and the four α -diversity indices exhibited no difference across the diverse groups (Fig. 4A–F), which indicate that DHEA treatment or tempol intervention has no obvious effect on the α -diversity of gut microbiota.

Next, we used the unweighted pair group method with arithmetic mean (UPGMA) clustering method, unweighted principal coordinate analysis (PCoA), and unweighted distance matrices (nonmetric multi-dimensional scaling [NMDS]) to assess the β -diversity of gut microbiota across diverse groups. The UPGMA clustering method classified the control and PCOS rat samples into two distinct groups, which suggest that the gut microbial profile was different between the PCOS rats and control rats. Although the DHEA + tempol group could not be separated completely from the DHEA + PBS group, it was somewhat dissimilar to the DHEA + PBS group, which indicate that tempol administration affects the gut microbial profile of the PCOS rats (Fig. 4G). The PCoA and NMDS analyses further revealed that the overall gut microbial compositions in the three rat groups were different (Fig. 4H–I), and the PermutMANOVA/ANOSIM analysis suggested that the differences among these groups were significant (Fig. 4J). Together, these results suggest that β -diversity of gut microbiota is affected by DHEA and tempol treatment.

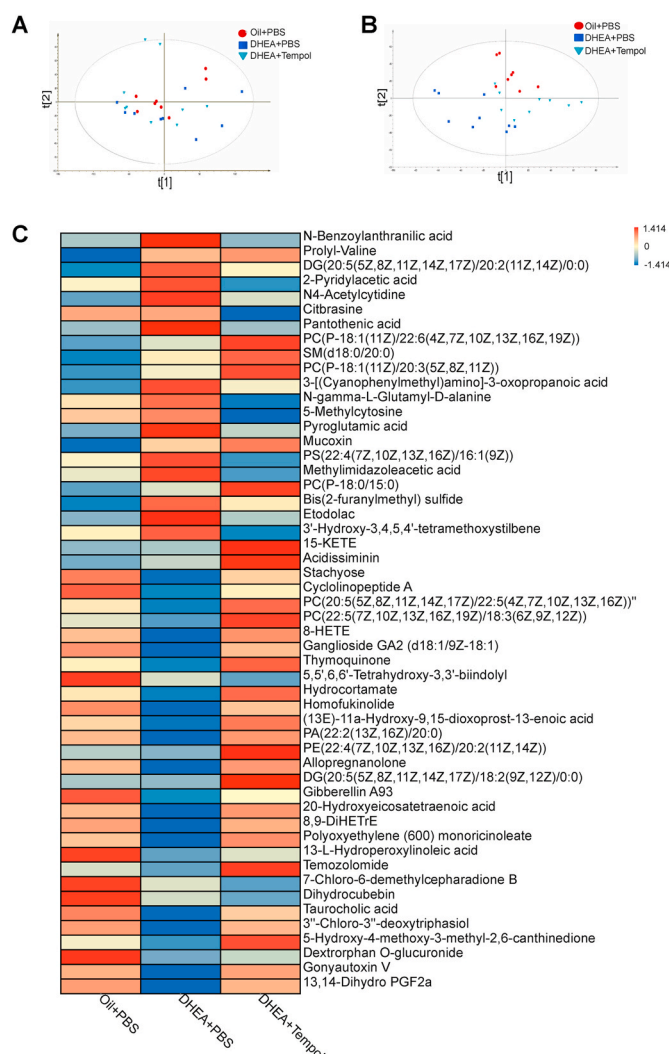


Fig. 6. Tempol affects serum metabolomic profiles. Score scatter plot for the principal component analysis (PCA) model indicated that most of the samples are in 95% Hotelling's T-squared ellipse. The abscissa and ordinate represent the scores of the first and second principal components, respectively. The color and shape of scatter points represent the experimental grouping of samples (A). The orthogonal variables irrelevant to the categorical variables in the metabolites were excluded through orthogonal projections to latent structures-discriminant analysis (OPLS-DA). The abscissa represents the predicted score of the first principal component, whereas the ordinate represents the score of the orthogonal principal component (B). An average heat map of the hierarchical clustering analysis for the three groups is presented. Abscissas represent different experimental groups, ordinates represent different metabolites, and different colors represent the relative expression of metabolites at the corresponding position. $N = 8-9$ rats per group. (For interpretation of the references to color in this figure legend, the reader is referred to the Web version of this article.)

To identify the key phylotypes that were significantly altered by DHEA and tempol treatments, all the validated sequences were analyzed using the linear discriminant analysis (LDA) effect size (LEfSe) method. The *Desulfovibrionaceae* genus was enriched in the oil + PBS group, whereas the *Muribaculaceae* and *Alloprevotella* genera were enriched in the DHEA + PBS and DHEA + tempol groups, respectively (Fig. 5A and B), which indicate that tempol could reshape the microbial structure of gut microbiota in PCOS rats.

The overall composition of gut microbiota across the three groups was further compared by analyzing the degree of bacterial taxonomic similarity at the phylum and genus levels. At the phylum level, *Firmicutes*

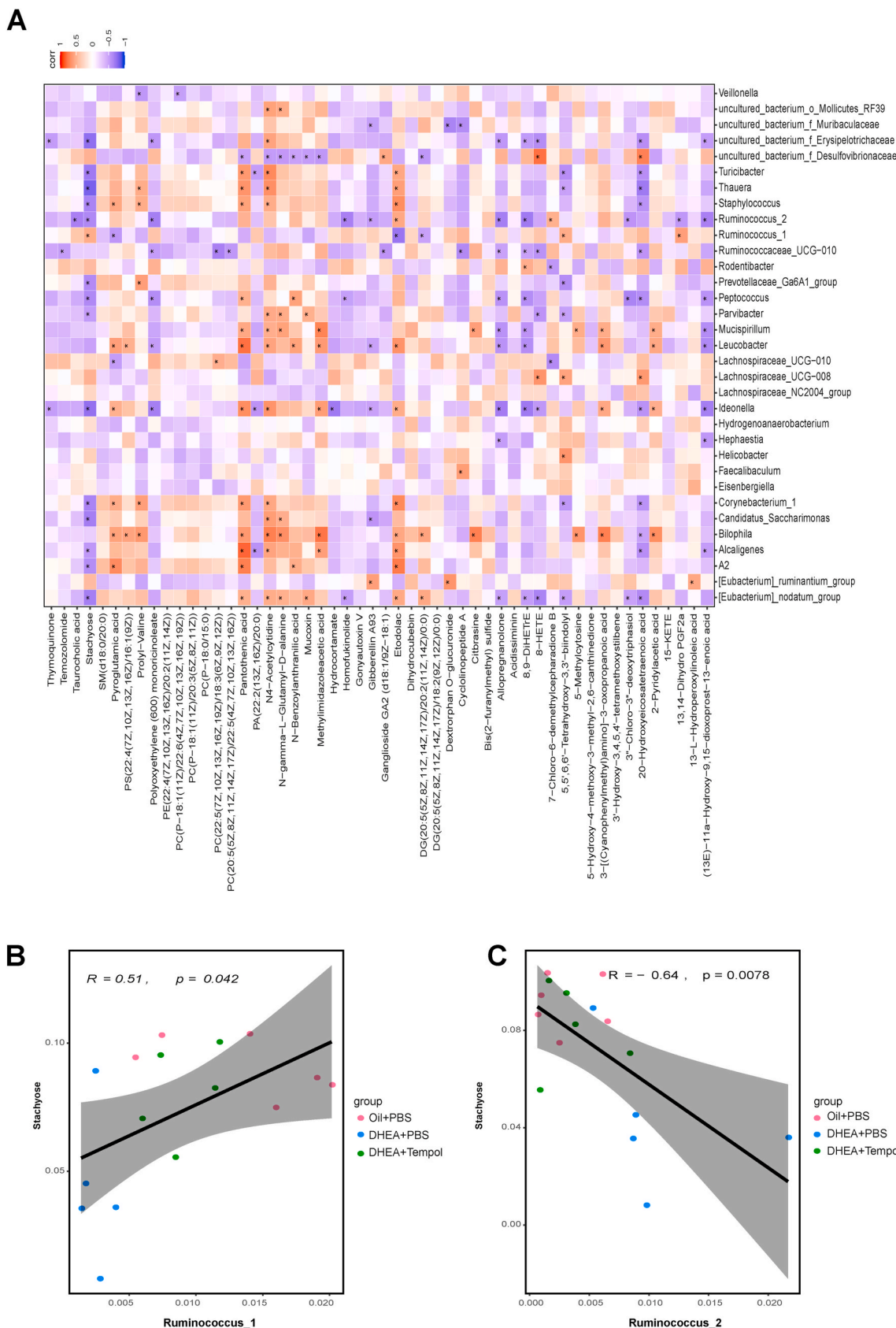


Fig. 7. Associations between gut microbial species and circulating metabolites. Spearman's rank correlation between 33 gut microbial species and 52 metabolites in the oil + PBS ($N = 8$), DHEA + PBS ($N = 9$), and DHEA + Tempol ($N = 9$) groups is presented (A). Red cells represent positive correlations between bacterial species and metabolites, and blue cells represent negative correlations between bacterial species and metabolites. * indicates that the correlation was significant. Scatter plot indicates the Person's correlation coefficient with statistical significance ($p < 0.05$) between *Ruminococcus_1* or *Ruminococcus_2* and serum

stachyose levels in all the three groups (B, C). (For interpretation of the references to color in this figure legend, the reader is referred to the Web version of this article.)

and *Bacteroidetes* were the dominant phyla among the three groups (Fig. 5C). DHEA treatment increased the abundance of *Actinobacteria*, *Bacteroidetes*, *Patescibacteria*, *Tenericutes*, and *Verrucomicrobia*, and decreased the number of *Epsilonbacteraeota* and *Proteobacteria*. However, the changes in the fraction of *Actinobacteria*, *Patescibacteria*, *Proteobacteria*, and *Tenericutes* were attenuated by tempol intervention (Fig. 5D). At the genus level, the *Lachnospiraceae_NK4A136_group* and *Mutibaculaceae* were dominant genera (Fig. 5E). The abundance of 33 genera was found to be significantly changed in response to DHEA or tempol treatment (Fig. S5). Specifically, DHEA considerably increased the abundance of *Thauera*, *Staphylococcus*, *Ideonella*, *Corynebacterium*, and *Ruminococcus_2*, and decreased the abundance of *Ruminococcus_1*. These changes were counteracted by tempol administration (Fig. 5F).

3.5. Associations between gut microbiota and circulating metabolites

Non-targeted metabolomics approaches were performed to measure

the serum metabolites in all the three groups and to investigate the association between gut microbiome and circulating metabolites in the host. The principal component analysis (PCA) revealed that the primary metabolic components were significantly different between the three groups (Fig. 6A). The supervised orthogonal projections to latent structures-discriminant analysis (OPLS-DA) score plot also exhibited a clear separation between the control and PCOS rats, and between the DHEA + PBS and DHEA + tempol groups (Fig. 6B). The relative abundances of 52 serum metabolites (including 26 lipids and lipid-like molecules) in the three groups were listed in Fig. 6C, which demonstrated that the abundances of most of serum metabolites in PCOS rats were totally different from those of control rats, indicating DHEA treatment has a profound effect on serum metabolic profiles. Tempol administration in PCOS rats also caused dramatic changes in the abundance of serum metabolites. Specially, the changes in the abundances of 28 serum metabolites caused by DHEA treatment were partially attenuated by tempol administration (Fig. 6C). For example, the abundances

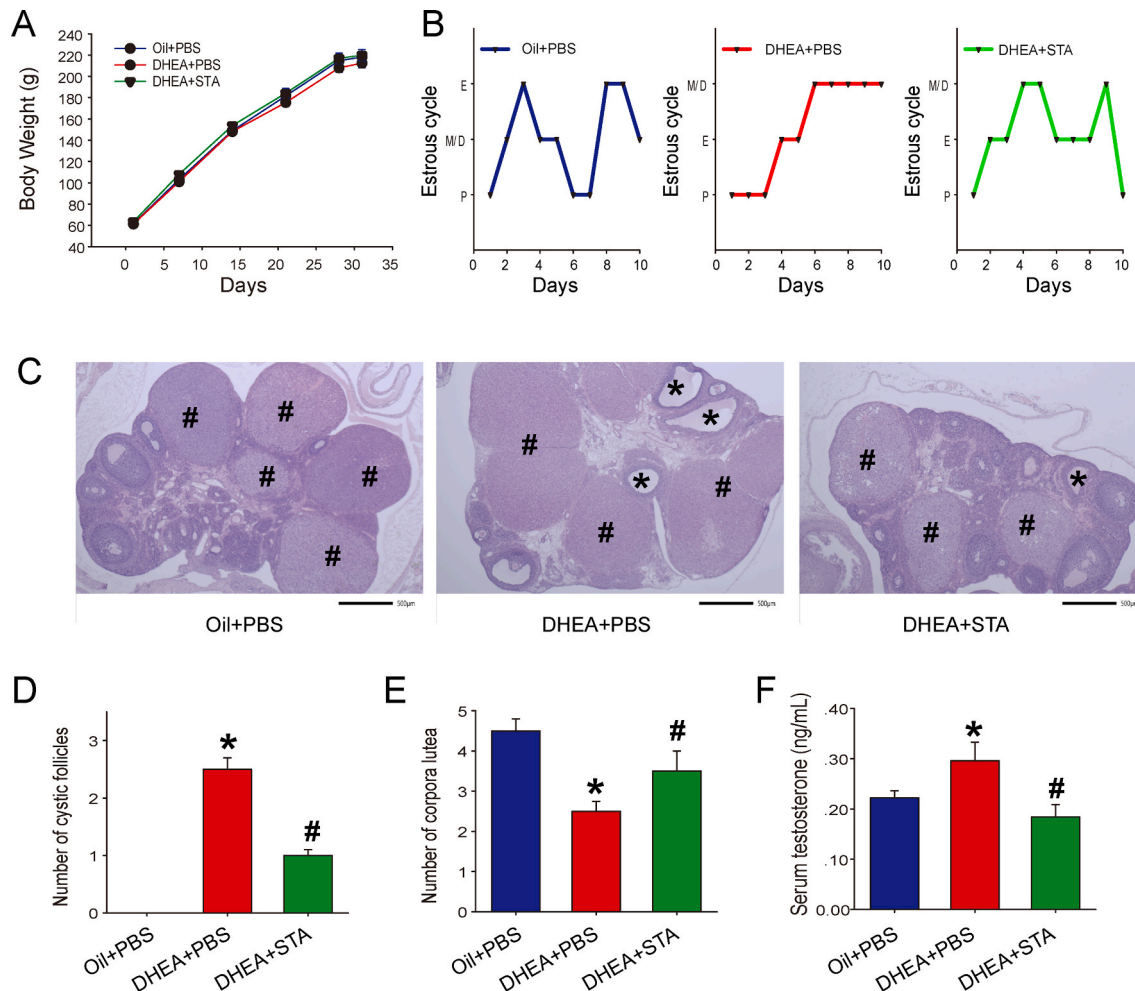


Fig. 8. Stachyose improved ovarian dysfunction in DHEA-induced PCOS rats. Female rats were randomly divided into three groups: oil + PBS ($N = 9$), DHEA + PBS ($N = 11$), DHEA + stachyose (STA) ($N = 11$). After treatment with DHEA or sesame oil for 21 days, female rats were administrated with PBS or 200 mg/kg stachyose for another 12 day. During the experiment period, body weight of rats was measured every week (A). The estrous cycles were determined after another 10 days ($N = 3$) (B). Representative ovary sections were stained with H&E (scale bar = 500 μm ; * indicates cystic follicles; # indicates corpora lutea) (C) and the number of cystic follicles (D) and corpora lutea (E) was determined from these stained sections ($N = 4$). Serum testosterone levels were measured using radioimmunoassay method (F) ($N = 7$). Data are presented as mean \pm SEM; * indicates significance ($p < 0.05$) compared with the oil + PBS group, # indicates significance ($p < 0.05$) compared with the DHEA + PBS group.

of stachyose, taurocholic acid, cyclolinoptide A and homofukinolide were decreased, whereas the abundances of DG (20:5(5Z,8Z,11Z,14Z,17Z)/20:2(11Z,14Z)/0:0), 3-[(Cyanophenylmethyl)amino]-3-oxopropanoic acid, Bis(2-furanylmethyl) sulfide and N4-Acetylcytidine were increased in the PCOS rats. After tempol administration, these changes were diminished.

The link between the abundances of circulating metabolites and gut microbiota in all three groups was investigated by performing the Spearman analysis to test the association between 33 genera and 52 metabolites (Fig. 7A). There were 11 metabolites which were not significantly correlated with any genus, including SM(d18:0/20:0), glycerophospholipids (PE(22:4(7Z,10Z,13Z,16Z)/20:2(11Z,14Z)), PC(P-18:1(11Z)/20:3(5Z,8Z,11Z)), PC(P-18:0/15:0)), DG(20:5(5Z,8Z,11Z,14Z,17Z)/18:2(9Z,12Z)/0:0), gonyautoxin V, dihydrocubebin, etc. Other glycerophospholipids (PC(P-18:1(11Z)/22:6(4Z,7Z,10Z,13Z,16Z,19Z)), PC(22:5(7Z,10Z,13Z,16Z,19Z)/18:3(6Z,9Z,12Z)), PC(20:5(5Z,8Z,11Z,14Z,17Z)/22:5(4Z,7Z,10Z,13Z,16Z)) were only significantly correlated with one or two genera, while polyunsaturated fatty acids (8-HETE, 8, 9-DiHETrE, 20-hydroxyeicosatetraenoic acid) were significantly correlated with at least 7 genera. Pantothenic acid, also known as vitamin B5, was significantly correlated with 13 genera. Stachyose, a functional oligosaccharide, was significantly correlated with 15 genera, including [*Eubacterium*] *nodontum* group, *A2*, *Alcaligenes*, *Candidatus_Saccharimonas*, *Corynebacterium_1*, *Ideonella*, *Parvibacter*, *Peptococcus*, *Prevotellaceae_Ga6A1_group*, *Ruminococcus_1*, *Ruminococcus_2*, *Staphylococcus*, *Thauera*, *Turicibacter*, and *f_Erysipelotrichaceae*. Moreover, the correlation between serum stachyose and *Ruminococcus_1* or *Ruminococcus_2* was further visualized using a scatter plot (Fig. 7B-C), which demonstrated that the decreased abundance of *Ruminococcus_1* and increased abundance of *Ruminococcus_2* were associated with lower serum stachyose levels in PCOS rats. When the abundances of *Ruminococcus_1* and *Ruminococcus_2* were changed by tempol intervention, serum stachyose levels were increased in PCOS rats.

3.6. Stachyose attenuates ovarian dysfunction in DHEA-induced PCOS rats

To determine whether stachyose is involved in the beneficial effects of tempol in PCOS rats, DHEA-treated rats were administered with 200 mg/kg stachyose for 12 days. Stachyose administration had no obvious effect on bodyweight (Fig. 8A), whereas improved estrous cycles disorders in PCOS rats (Fig. 8B). H&E staining further demonstrated that stachyose administration decreased the number of cystic follicles and increased the formation of corpus lutea in ovaries (Fig. 8C-E). Stachyose also significantly attenuated the increases in serum testosterone levels in PCOS rats (Fig. 8F). Together, these results suggest that stachyose really improved ovarian dysfunction and ameliorated pathological damage of ovarian tissues in PCOS rats.

4. Discussion

The present study has two major new findings. First, tempol is effective in attenuating DHEA-induced ovarian dysfunction in PCOS rats. Second, the protective effect of tempol in PCOS rats is associated with the ameliorated intestinal oxidative stress, attenuated gut dysbiosis and restored circulating metabolite profile, which indicate that tempol prevents PCOS by scavenging superoxide and modulating the gut microbiota.

As a well-known SOD mimetic, tempol protects against numerous oxidative stress-related diseases, such as hypertension [27], obesity [28, 29], insulin resistance [30] and pancreatic injury [31]. Tempol can also reduce ovarian ischemia-reperfusion (I/R) injury in female Wistar albino rats [32]. Emerging evidence suggests that oxidative stress contributes greatly to the PCOS pathophysiology [33,34]. Thus, tempol could be a potential therapeutic drug for PCOS. In the present study, we

observed that tempol ameliorated estrous cycles disorders, ovarian morphology disruption, increased serum testosterone levels, and cell apoptosis in DHEA-treated rats, which suggest that tempol could improve ovarian dysfunction in PCOS rats. Our results concurred with other previous studies that demonstrated the beneficial effects of antioxidant supplementation on patients with PCOS [10,35].

Numerous studies have demonstrated that the protective effect of tempol is associated with its ability to scavenge oxygen free radicals and reduce oxidative stress in target organs [36]. Interestingly, we observed no effect of tempol administration on the levels of MDA, 3'-NT, AGEs and T-AOC, activity of Gpx and SOD, and SOD1 and SOD2 protein expression in the ovaries of DHEA-treated rats. However, we observed that tempol attenuated the systemic oxidative stress in PCOS rats. Moreover, tempol had a profound effect on intestinal oxidative stress, as evidenced by the reduced MDA, 3'-NT and AGEs levels and increased SOD1 and SOD2 expressions in the intestinal tract. Therefore, the protective effect of tempol on DHEA-induced ovarian dysfunction was not attributed to reduced oxidative stress in ovaries, and the intestinal tissue might be considered the direct target of tempol. Similar results were also observed in obese mice, where tempol improved the metabolic profile by inhibiting intestinal FXR signaling and altering the gut microbiome [25].

Although our data identified a novel target organ for tempol in PCOS rats, the mechanism by which tempol protects against ovarian dysfunction and metabolic abnormality remains unclear. The occurrence of microbiota dysbiosis occurs in patients with PCOS [15,37] and the PCOS animal models [18,38] is well-established, and alternations in the abundance of specific types of the gut bacteria have been associated with clinical manifestations of PCOS [19]. For example, a study by Qi et al. demonstrated that the abundance of *Bacteroides_vulgatus* is significantly increased in the gut microbiota of patients with PCOS and that the transplantation of fecal microbiota from PCOS women or *B.vulgatus*-colonized recipient mice caused metabolic abnormality and ovarian dysfunction in mice [15]. On the other hand, restoration of dysbiosis by supplementation with probiotics, and synbiotics or transplantation of fecal microbiota from healthy controls might provide new directions to the PCOS treatment [39-41]. In the present study, significant differences were observed in gut microbial compositions between the control and DHEA-treated rats, and most of these differences were diminished by tempol treatment. At the phylum level, tempol restores gut dysbiosis by downregulating *Actinobacteria*, *Patescibacteria* and *Tenericutes*, and by upregulating *Proteobacteria*. At the genus level, tempol increased the abundance of *Ruminococcus_1* and decreased the abundances of *Thauera*, *Staphylococcus*, *Ideonella*, *Corynebacterium*, and *Ruminococcus_2* in PCOS rats. Therefore, tempol may ameliorated PCOS in rats (at least partially) by improving the gut microbiota.

The gut microbiota affects host metabolism by interacting with host signaling pathways. For example, the elevated level of *B.vulgatus* in the gut microbiota of patients with PCOS was accompanied by a reduction in glycodeoxycholic acid (GDCA) and tauroursodeoxycholic acid (TUDCA) levels [15]. These bile acids are the signaling molecules that regulate glucose metabolism and insulin sensitivity through FXR and G protein-coupled bile acid receptor 1 (GPBAR1). Ursodeoxycholic acid (UDCA) treatment improves ovarian morphology and decreases total testosterone and insulin levels [42]. Moreover, GDCA induces intestinal group 3 innate lymphoid cell IL-22 secretion, and IL-22 in turn improves the PCOS phenotype [15]. Tempol treatment in obese mice significantly increased bile acid levels in feces and intestinal tissue by reducing the abundance of genus *Lactobacillus* and its bile salt hydrolase activity [25]. Tempol also attenuated the reduction in the serum bile acid levels in the present study. Specifically, alternations in serum taurocholic acid levels were negatively correlated with the abundance of *Ruminococcus_2*. However, further studies are required to elucidate the precise mechanism by which tempol affects bile acid metabolism in PCOS rats.

A significant correlation between serum stachyose levels and the abundances of 15 genera in the gut microbiota suggests that stachyose

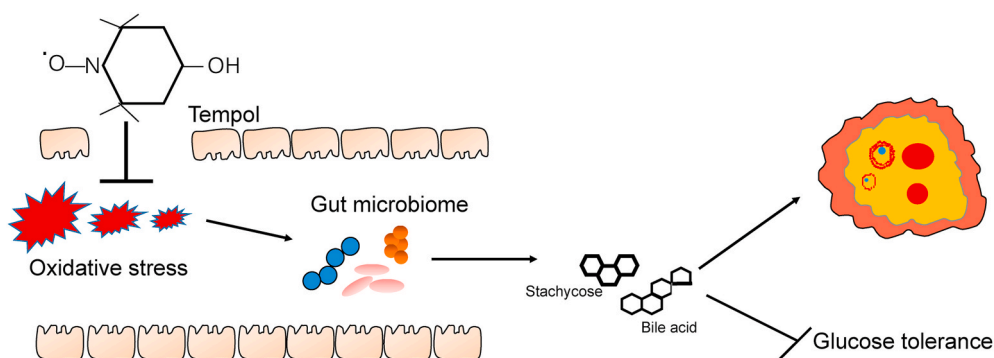


Fig. 9. Diagram of the potential signaling pathway involved in ameliorates glucose tolerance and polycystic ovary.

might be another major host metabolite that interacts with gut microbiota. Stachyose functions as a form of natural probiotic and exerts beneficial effects on multiple diseases through the modulation of gut microbiota [43–45]. For example, stachyose alleviates dextran sulfate sodium-induced acute colitis by increasing *Akkermansia* [43]. In HFD-fed mice, stachyose intervention diminished colonic and hepatic inflammation, which was associated with improved gut microbiota dysbiosis [45]. Moreover, stachyose possesses antioxidant properties. The rate constant for the reaction between stachyose and hydroxyl radicals is higher than those of galactinol, raffinose and typical antioxidants, such as ascorbate and glutathione (GSH) [46]. Oral administration of raffinose family oligosaccharides, mainly composed of stachyose (61.7%, w/w), significantly increased hepatic GSH, GSH-peroxidase, SOD, and T-AOC levels, and ameliorated CCL₄-induced hepatic oxidative stress in mice [47]. In the present study, the serum stachyose levels were positively correlated with the abundance of *Ruminococcus_1* and negatively correlated with the abundance of *Ruminococcus_2* in all the three rat groups. Tempol treatment increased serum stachyose levels in PCOS rats, which was associated with an increase in the abundance of *Ruminococcus_1* and decrease in the abundance of *Ruminococcus_2*. Moreover, stachyose administration improved ovarian dysfunction in PCOS rats. Considering the potential beneficial effect of stachyose on health, we proposed that the protective effect of tempol on PCOS is also related to the modulation of the interaction between gut microbiota and stachyose.

In summary, tempol protects against DHEA-induced PCOS syndrome by decreasing intestinal oxidative stress, restoring gut dysbiosis, and modulating the interaction between gut microbiota and host metabolites (Fig. 9). These results suggest that tempol administration is a potential therapeutic strategy for PCOS.

Declaration of competing interest

No competing financial interests exist.

Acknowledgement

This study was supported by grants from the National Natural Science Foundation of China (81801407, 82070250), Beijing Natural Science Foundation (7184212), Beijing Hospitals Authority Youth Programme (QML20191401) and Beijing Postdoctoral Research Foundation.

We thank TopEdit (www.topedit.com) for its linguistic assistance during the preparation of this manuscript.

Appendix A. Supplementary data

Supplementary data to this article can be found online at <https://doi.org/10.1016/j.redox.2021.101886>.

References

- [1] R.J. Norman, D. Dewailly, R.S. Legro, T.E. Hickey, Polycystic ovary syndrome, *Lancet* (London, England) 370 (9588) (2007) 685–697.
- [2] H.J. Teede, M.L. Misso, M.F. Costello, A. Dokras, J. Laven, L. Moran, T. Piltonen, R. J. Norman, Recommendations from the international evidence-based guideline for the assessment and management of polycystic ovary syndrome, *Hum. Reprod. (Oxf.)* 33 (9) (2018) 1602–1618.
- [3] R. Azziz, E. Carmina, Z. Chen, A. Dunaif, J.S. Laven, R.S. Legro, D. Lizneva, B. Natterson-Horowitz, H.J. Teede, B.O. Yildiz, Polycystic ovary syndrome, *Nat. Rev. Dis. Prim.* 2 (2016) 16057.
- [4] D.A. Dumesic, S.E. Oberfield, E. Stener-Victorin, J.C. Marshall, J.S. Laven, R. S. Legro, Scientific statement on the diagnostic criteria, epidemiology, pathophysiology, and molecular genetics of polycystic ovary syndrome, *Endocr. Rev.* 36 (5) (2015) 487–525.
- [5] K.M. Barkath Nisha Hyderali, Oxidative stress and cardiovascular complications in polycystic ovarian syndrome, *Eur. J. Obstet. Gynecol. Reprod. Biol.* 191 (2015) 15–22.
- [6] U.V.V. PApalou, E. Diamanti-Kandarakis, Oxidative stress in polycystic syndrome, *Curr. Pharmaceut. Des.* 22 (18) (2016) 2709–2722.
- [7] F.K.S. masjedi, F. Agah, N. Karbalaei, Association between sex steroids and oxidative status with vitamin D levels in follicular fluid of non-obese PCOS and healthy women, *J. Reproduction Infertil.* 20 (3) (2019) 132–142.
- [8] Y. Sun, S. Li, H. Liu, Y. Gong, H. Bai, W. Huang, Q. Liu, L. Guan, P. Fan, Association of GPx1 P198L and CAT C-262T genetic variations with polycystic ovary syndrome in Chinese women, *Front. Endocrinol.* 10 (2019) 771.
- [9] E.E. Bafor, A.P. Uchendu, O.E. Osayande, O. Omoruyi, U.G. Omigiade, E. E. Panama, O.O. Elekofehinti, E.L. Oragwuncha, A. Momodu, Ascorbic Acid and Alpha-Tocopherol Contribute to the Therapy of Polycystic Ovarian Syndrome in Mouse Models, *Reproductive sciences, Thousand Oaks, Calif.*, 2020.
- [10] A. Izadi, S. Shirazi, S. Taghizadeh, B.P. Gargari, Independent and additive effects of coenzyme Q10 and vitamin E on cardiometabolic outcomes and visceral adiposity in women with polycystic ovary syndrome, *Arch. Med. Res.* 50 (2) (2019) 1–10.
- [11] A. Izadi, S. Ebrahimi, S. Shirazi, S. Taghizadeh, M. Parizad, L. Farzadi, B.P. Gargari, Hormonal and metabolic effects of coenzyme Q10 and/or vitamin E in patients with polycystic ovary syndrome, *J. Clin. Endocrinol. Metabol.* 104 (2) (2019) 319–327.
- [12] G. Kyei, A. Sobhani, S. Nekonom, M. Shabani, F. Ebrahimi, M. Qasemi, E. Salahi, A. Fardin, Assessing the effect of MitoQ(10) and Vitamin D3 on ovarian oxidative stress, steroidogenesis and histomorphology in DHEA induced PCOS mouse model, *Heliyon* 6 (7) (2020), e04279.
- [13] J. Chen, Q. Guo, Y.H. Pei, Q.L. Ren, L. Chi, R.K. Hu, Y. Tan, Effect of a short-term vitamin E supplementation on oxidative stress in infertile PCOS women under ovulation induction: a retrospective cohort study, *BMC Wom. Health* 20 (1) (2020) 69.
- [14] C.S. Wilcox, Effects of tempol and redox-cycling nitroxides in models of oxidative stress, *Pharmacol. Therapeut.* 126 (2) (2010) 119–145.
- [15] X. Qi, C. Yun, L. Sun, J. Xia, Q. Wu, Y. Wang, L. Wang, Y. Zhang, X. Liang, L. Wang, et al., Gut microbiota-bile acid-interleukin-22 axis orchestrates polycystic ovary syndrome, *Nat. Med.* 25 (8) (2019) 1225–1233.
- [16] Y. Liang, Q. Ming, J. Liang, Y. Zhang, H. Zhang, T. Shen, Gut microbiota dysbiosis in Polycystic ovary syndrome (PCOS): association with obesity - a preliminary report, *Can. J. Physiol. Pharmacol.* 98 (11) (2020) 803–809.
- [17] J. Xue, X. Li, P. Liu, K. Li, L. Sha, X. Yang, L. Zhu, Z. Wang, Y. Dong, L. Zhang, et al., Inulin and metformin ameliorate polycystic ovary syndrome via anti-inflammation and modulating gut microbiota in mice, *Endocr. J.* 66 (10) (2019) 859–870.
- [18] T. Wang, L. Sha, Y. Li, L. Zhu, Z. Wang, K. Li, H. Lu, T. Bao, L. Guo, X. Zhang, et al., Dietary α -linolenic acid-rich flaxseed oil exerts beneficial effects on polycystic ovary syndrome through sex steroid hormones-microbiota-inflammation Axis in rats, *Front. Endocrinol.* 11 (2020) 284.
- [19] F.F. He, Y.M. Li, Role of gut microbiota in the development of insulin resistance and the mechanism underlying polycystic ovary syndrome: a review, *J. Ovarian Res.* 13 (1) (2020) 73.
- [20] V.G. Thackray, Sex, microbes, and polycystic ovary syndrome, *Trends Endocrinol. Metabol.: TEM (Trends Endocrinol. Metab.)* 30 (1) (2019) 54–65.

- [21] M.K.A. Gyuraszova, R. Gardlik, Association between oxidative status and the composition of intestinal microbiota along the gastrointestinal tract, *Med. Hypotheses* 103 (2017) 81–85.
- [22] J. Xie, W. Song, X. Liang, Q. Zhang, Y. Shi, W. Liu, X. Shi, Protective effect of quercetin on streptozotocin-induced diabetic peripheral neuropathy rats through modulating gut microbiota and reactive oxygen species level, *Biomed. & Pharmacother. = Biomedecine & pharmacotherapie* 127 (2020), 110147.
- [23] A. Ortega-Hernández, E. Martínez-Martínez, R. Gómez-Gordo, N. López-Andrés, A. Fernández-Celis, B. Gutiérrez-Miranda, M.L. Nieto, T. Alarcón, C. Alba, D. Gómez-Garre, et al., The interaction between mitochondrial oxidative stress and gut microbiota in the cardiometabolic consequences in diet-induced obese rats, *Antioxidants* 9 (7) (2020).
- [24] A.M. El-Baz, A.E. Khodir, M.M. Adel El-Sokkary, A. Shata, The protective effect of *Lactobacillus* versus 5-aminosalicylic acid in ulcerative colitis model by modulation of gut microbiota and Nrf2/Ho-1 pathway, *Life Sci.* 256 (2020), 117927.
- [25] F. Li, C. Jiang, K.W. Krausz, Y. Li, I. Albert, H. Hao, K.M. Fabre, J.B. Mitchell, A. D. Patterson, F.J. Gonzalez, Microbiome remodelling leads to inhibition of intestinal farnesoid X receptor signalling and decreased obesity, *Nat. Commun.* 4 (2013) 2384.
- [26] T. Li, R. Feng, C. Zhao, Y. Wang, J. Wang, S. Liu, J. Cao, H. Wang, T. Wang, Y. Guo, et al., Dimethylarginine dimethylaminohydrolase 1 protects against high-fat diet-induced hepatic steatosis and insulin resistance in mice, *Antioxidants Redox Signal.* 26 (11) (2017) 598–609.
- [27] S.F.Y.J. Knight, S. Roy, J.D. Imig, Simvastatin and tempol protect against endothelial dysfunction and renal injury in a model of obesity and hypertension, *Am. J. Physiol. Ren. Physiol.* 298 (1) (2010) 86–94.
- [28] M.K.K. Yamato, Y. Yamanaka, M. Saiga, K. Yamada, TEMPOL increases NAD(+) and improves redox imbalance in obese mice, *Redox Biol* 8 (2016) 316–322.
- [29] C.H.M.J. Kim, C.A. Bursill, A.L. Sowers, A. Thetford, J.A. Cook, D.M. van Reyk, M. J. Davies, The nitroxide radical TEMPOL prevents obesity, hyperlipidaemia, elevation of inflammatory cytokines, and modulates atherosclerotic plaque composition in apoE^{-/-} mice, *Atherosclerosis* 240 (1) (2015) 234–241.
- [30] F.B.H. Bourgoin, M. Badaeu, R. Larivière, A. Nadeau, M. Pitre, Effects of tempol on endothelial and vascular dysfunctions and insulin resistance induced by a high-fat high-sucrose diet in the rat, *Can. J. Physiol. Pharmacol.* 91 (7) (2013) 547–561.
- [31] Y. Wang, L. Ai, B. Hai, Y. Cao, R. Li, H. Li, Y. Li, Tempol alleviates chronic intermittent hypoxia-induced pancreatic injury through repressing inflammation and apoptosis, *Physiol. Res.* 68 (3) (2019) 445–455.
- [32] N. Pinar, O. Soyulu Karapınar, O. Özcan, E. Atik Doğan, S. Bayraktar, Protective effects of tempol in an experimental ovarian ischemia-reperfusion injury model in female Wistar albino rats, *Can. J. Physiol. Pharmacol.* 95 (7) (2017) 861–865.
- [33] X. Zeng, Q. Huang, S.L. Long, Q. Zhong, Z. Mo, Mitochondrial dysfunction in polycystic ovary syndrome, *DNA Cell Biol.* 39 (8) (2020) 1401–1409.
- [34] M. Mohammadi, Oxidative stress and polycystic ovary syndrome: a brief review, *Int. J. Prev. Med.* 10 (2019) 86.
- [35] J. Heshmati, F. Golab, M. Morvaridzadeh, E. Potter, M. Akbari-Fakhrabadi, F. Farsi, S. Tanbakooei, F. Shidfar, The effects of curcumin supplementation on oxidative stress, Sirtuin-1 and peroxisome proliferator activated receptor γ coactivator 1 α gene expression in polycystic ovarian syndrome (PCOS) patients: a randomized placebo-controlled clinical trial, *Diabetes & Metabol. Syndr.* 14 (2) (2020) 77–82.
- [36] Z.W.C. Ge, J. Zhang, X. Li, J. Hu, Tempol protects against acetaminophen induced acute hepatotoxicity by inhibiting oxidative stress and apoptosis, *Front. Physiol.* 31 (10) (2019) 660.
- [37] R. Liu, C. Zhang, Y. Shi, F. Zhang, L. Li, X. Wang, Y. Ling, H. Fu, W. Dong, J. Shen, et al., Dysbiosis of gut microbiota associated with clinical parameters in polycystic ovary syndrome, *Front. Microbiol.* 8 (2017) 324.
- [38] S.T. Kelley, D.V. Skarra, A.J. Rivera, V.G. Thackray, The gut microbiome is altered in a letrozole-induced mouse model of polycystic ovary syndrome, *PLoS One* 11 (1) (2016), e0146509.
- [39] S. Ahmadi, M. Jamilian, M. Karamali, M. Tajabadi-Ebrahimi, P. Jafari, M. Taghizadeh, M.R. Memarzadeh, Z. Asemi, Probiotic supplementation and the effects on weight loss, glycaemia and lipid profiles in women with polycystic ovary syndrome: a randomized, double-blind, placebo-controlled trial, *Hum. Fertil.* 20 (4) (2017) 254–261.
- [40] J. Zhang, Z. Sun, S. Jiang, X. Bai, C. Ma, Q. Peng, K. Chen, H. Chang, T. Fang, H. Zhang, Probiotic bifidobacterium lactis V9 regulates the secretion of sex hormones in polycystic ovary syndrome patients through the gut-brain axis, *mSystems* 4 (2) (2019).
- [41] Y. Guo, Y. Qi, X. Yang, L. Zhao, S. Wen, Y. Liu, L. Tang, Association between polycystic ovary syndrome and gut microbiota, *PLoS One* 11 (4) (2016), e0153196.
- [42] I. Gozukara, R. Dokuyucu, T. Özgür, O. Özcan, N. Pinar, R.K. Kurt, S.K. Kucur, K. Dolapcioglu, Histopathologic and metabolic effect of ursodeoxycholic acid treatment on PCOS rat model, *Gynecol. Endocrinol. : Off. J. Int. Soc. Gynecol. Endocrinol.* 32 (6) (2016) 492–497.
- [43] L. He, F. Zhang, Z. Jian, J. Sun, J. Chen, V. Liapao, Q. He, Stachyose modulates gut microbiota and alleviates dextran sulfate sodium-induced acute colitis in mice, *Saudi J. Gastroenterol. : Off. J. Saudi Gastroenterol. Assoc.* 26 (3) (2020) 153–159.
- [44] G. Liu, J. Bei, L. Liang, G. Yu, L. Li, Q. Li, Stachyose improves inflammation through modulating gut microbiota of high-fat diet/streptozotocin-induced type 2 diabetes in rats, *Mol. Nutr. Food Res.* 62 (6) (2018), e1700954.
- [45] Y. Liu, T. Li, A. Alim, D. Ren, Y. Zhao, X. Yang, Regulatory effects of stachyose on colonic and hepatic inflammation, gut microbiota dysbiosis, and peripheral CD4(+) T cell distribution abnormality in high-fat diet-fed mice, *J. Agric. Food Chem.* 67 (42) (2019) 11665–11674.
- [46] A. Nishizawa-Yokoi, Y. Yabuta, S. Shigeoka, The contribution of carbohydrates including raffinose family oligosaccharides and sugar alcohols to protection of plant cells from oxidative damage, *Plant Signal. Behav.* 3 (11) (2008) 1016–1018.
- [47] R.Z.Y. Zhang, Y. Sun, X. Lu, X. Yang, Isolation, characterization, and hepatoprotective effects of the raffinosefamily oligosaccharides from *Rehmannia glutinosa* Libosch, *J. Agric. Food Chem.* 61 (32) (2013) 7786–7793.